Shocks in asymmetric simple exclusion processes of interacting particles

Sutapa Mukherji
Department of Physics, Indian Institute of Technology, Kanpur 208 016, India
(Received 8 October 2006; revised manuscript received 30 January 2007; published 31 July 2007)

In this paper, we study shocks and related transitions in asymmetric simple exclusion processes of particles with nearest-neighbor interactions. We consider two kinds of interparticle interactions. In one case, the particle-hole symmetry is broken due to the interaction. In the other case, particles have an effective repulsion due to which the particle current density drops down near one-half filling. These interacting particles move on a one-dimensional lattice which is open at both the ends with injection of particles at one end and withdrawal of particles at the other. In addition to this, there are possibilities of attachments or detachments of particles to or from the lattice with certain rates. The hydrodynamic equation that involves the exact particle current density of the particle conserving system and additional terms taking care of the attachment-detachment kinetics is studied using the techniques of boundary layer analysis.

DOI: 10.1103/PhysRevE.76.011127 PACS number(s): 05.40.−a, 02.50.Ey, 64.60.−i, 89.75.−k

I. INTRODUCTION

Asymmetric simple exclusion process (ASEP) comprises of particles performing biased hopping in a preferred direction on a one-dimensional chain. This biased hopping gives rise to a finite particle current due to which the detailed balance is violated. In its simplest version, the particles respect mutual exclusion due to which a lattice site cannot be occupied by more than one particle. Recently, ASEP with nonconservation of particles [1] have drawn a lot of attention because these systems have better resemblance with the motors participating in biological transports inside the cell [2] than the particle number conserving systems. The particles undergoing ASEP are analogous to the molecular motors performing directed motion on tracks laid by the biopolymers [1,3]. The conservation of particle number may be violated by absorption (or evaporation) of particles to (or from) the chain, a process, that is similar to the attachment or detachment of motors from the filament.

One of the important issues involving these nonequilibrium processes on an open system is the boundary induced phase transition [4]. Boundary induced phase transitions are possible for both particle conserving [5] and nonconserving ASEP [1,6–9] with the latter one having a richer phase diagram with new phases. The other important aspect which influences the phase diagram is the interaction between the particles in addition to the mutual exclusion [10]. These interactions affect the particle current along the lattice. Since the particle current carries the boundary information to the bulk, boundary induced phase transitions are likely to be affected by the change in the interparticle interaction.

The ASEP we consider here is defined on a one-dimensional lattice of size l with N lattice points [11]. Each site can be empty or occupied by a particle. A particle on site i can hop to site $i+1$ with unit rate provided the target site is empty. A steady flow of particles along this one-dimensional channel is maintained by injection and withdrawal of particles at certain rates at left and right ends of the lattice, respectively. The boundaries are coupled with particle reservoirs with fixed particle densities. We assume that the rates are such that the left and the right boundaries have particle densities α and γ, respectively. The particle number in the bulk is not conserved since the particles are allowed to detach (or attach) from (or to) the chain with rates ω_d (ω_a). In the steady state, depending on the values of α and γ, the system is found to exist in different phases that are characterized by the particle density ρ and the current density $j(\rho)$. These phases are represented in the phase diagram in the space of α and γ. Monte Carlo simulations and mean field analysis of this model [1,6] show low-density, high-density, and maximal-current phases in addition to a phase, known as the shock phase, where the low-density and high-density, regions coexist. The density profile across the lattice has a jump discontinuity (shock) from a low-density region to a high-density region. It has also been shown that the transition to the shock phase can become critical under special values of the boundary parameters [1]. Shocks (domain walls) separating different steady-state density profiles have been observed in ASEP without the absorption-desorption kinetics. However, in this case, the position of a shock on the lattice fluctuates and they can, in general, move on the lattice. The dynamics of such shocks [10,12] drive the system to settle in one of its steady states which are known as high-density, low-density, and maximal-current phases (in case of particles having only mutual exclusion). Studying the dynamics of such shocks helps in understanding the nature of the phase transitions in such systems. Unlike this particle conserving ASEP, here the shocks are localized [1,6] and there are stationary states in the phase diagram where the density profiles have such shocks. The shock is upward in the sense that the low-density phase appears on the left of the shock and the high-density phase appears on the right of the shock. The position of these stationary shocks is determined by α, γ and the absorption-desorption rates. A boundary layer analysis shows that the transition to the shock phase from a low-density phase can happen through a critical deconfinement of a boundary layer from the edge of the system [7]. In addition, it has been shown in a general way that this transition to the shock phase is associated with a dual transition [8,9]. The dual transition is a boundary transition across which the slope of the boundary layer changes sign with the shape of the bulk density profile remaining unchanged. These boundary and shock transition lines meet at the critical point. The presence of the dual transition helps in developing a general approach through which one can clas-

sify the phase diagrams into different categories. This has been done in Ref. [9] using the knowledge of zeros of a set of coarse-grained functions present in the equation describing the steady state density profile.

The effect of the interparticle interactions on the particle conserving ASEP has been found to be quite drastic [10]. Typically one considers interactions of the following nature [13]. The particles hop to the right with bulk hopping rates

$$0\ 1\ 0\ 0 \rightarrow 0\ 0\ 1\ 0 \quad \text{with rate } 1+\delta, \tag{1}$$

$$1\ 1\ 0\ 0 \rightarrow 1\ 0\ 1\ 0 \quad \text{with rate } 1+\Delta, \tag{2}$$

$$0\ 1\ 0\ 1 \rightarrow 0\ 0\ 1\ 1 \quad \text{with rate } 1-\Delta, \tag{3}$$

$$1\ 1\ 0\ 1 \rightarrow 1\ 0\ 1\ 1 \quad \text{with rate } 1-\delta. \tag{4}$$

Here, 1 and 0 imply an occupied and an unoccupied site, respectively. $\Delta=\delta=0$, is the case of ASEP with only mutual exclusion. In this case, the current density $j(\rho)=\rho(1-\rho)$ respects particle-hole symmetry and has a maximum at $\rho=1/2$. An exact solution of the particle conserving problem [5] reveals that there are primarily three phases known as the low-density, high-density, and the maximal-current phases. The case of $\Delta\rightarrow 1$ implies a repulsion among the particles due to which the current versus density plot is expected to show a minimum near the half-filling. In the range $0\leqslant\Delta\leqslant 1$, as Δ increases, the current density plot develops double maxima from a single maximum picture. With a minimum in the current versus density plot, the phase diagram contains a minimum-current phase [10] in addition to the low-density, high-density, and the maximal-current phases. At this minimum current phase, the bulk density has a value that corresponds to the minimum value of the current. The maximal-current phase, in general, is also expected to be of two different types in which the bulk density corresponds to two different maxima of the current. Equations (1) and (4) involving δ imply that the particle current is the same as the vacancy current for $\delta=0$. A finite δ breaks this equality since $\delta>0$ and $\delta<0$ imply larger particle or vacancy currents, respectively. This particle-hole asymmetry introduces an asymmetry in the current versus density plot.

Since the particle nonconservation and the interparticle interaction both individually leave significant impact on ASEP, their combined effect is expected to be interesting. Although the phase diagram of the particle nonconserving version of the interacting ASEP has not been probed, numerical simulations exhibit some new features such as downward shock (see Fig. 1) and double shocks [14] in the density profile. In case of downward shock, the shock is a discontinuity in the density profile separating a high-density part on the left and a low-density part on the right. The density profile with a double shock consists of two successive upward jumps separating a low-density part on the left and a high-density part on the right. The particular feature that interests us here is the downward shock in the density profile.

In this paper, we look into the details of the shocks for two limiting cases (i) $\Delta=0$ and $\delta=1$ and (ii) $\Delta=1$ and $\delta=0$ using a boundary layer analysis. These problems serve as the limiting cases of the most general interacting case which is technically more difficult to handle. The first case is useful for the verification of our earlier predictions related to shock-ening transition, dual boundary transition, and criticality. We show that although the shape of the density profile is different in this case, different phase transitions and the phase diagram are qualitatively the same as those of only the mutual exclusion case with $\omega_a\neq\omega_d$. Further, the asymmetry in the current versus density plot does not alter the exponents which remain the same as those of the pure mutual exclusion case with $\omega_a\neq\omega_d$. In the second case, our focus is particularly on the shape of the density profile that has a downward shock, location of the shock and specific conditions on the boundary parameters α and γ for which such shock can be observed. The aim is also to show how the earlier analysis for the upward shock can be appropriately modified to understand the details of the downward shock. We show that the earlier predictions [14] about the ranges in which the values of the densities at the upper and lower end of the shock must lie, are satisfied naturally in the boundary layer analysis. Although the boundary layer analysis presented here can be used to obtain other features such as phases with upward shocks, entire phase diagram with the details of the phase boundaries, we plan to present those with supportive numerical analysis of the system in a later presentation.

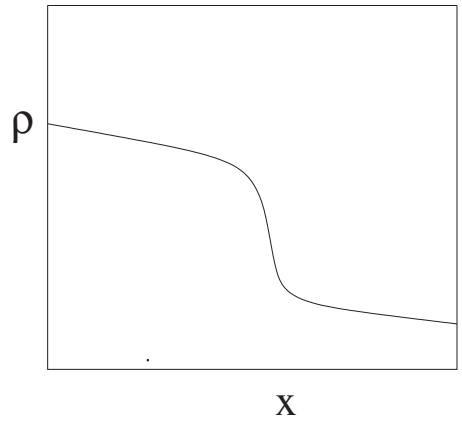

FIG. 1. A diagram for the density profile with a downward shock.

The paper is organized as follows. In the next section, we discuss some of the details of the model. A few basic principles of the boundary layer analysis are discussed in Sec. III. In Sec. IV, we consider the first case, namely that of $\Delta=0$ and $\delta=1$. Some results related to the density profiles and phase diagrams for this case are presented in the Appendix. In Sec. V, we consider the case of $\Delta=1$ and $\delta=0$. We conclude the paper with a brief summary of the main results in Sec. VI.

II. MODEL

In general, for a particle conserving system, one can write down a discrete continuity equation

$$\frac{d\rho_k}{dt}=j_{k-1}-j_k, \tag{5}$$

where j_k is the average current across the bond between the kth and $k-1$th sites and ρ_k is the average particle occupancy

at the kth site. The average current takes care of the particle hopping rule that is problem specific. In the presence of particle absorption-desorption kinetics, we may supplement this equation with other terms responsible for particle absorption and desorption. One can obtain a simple, solvable continuum model from the resulting equation by making a mean-field approximation that neglects particle correlations. In case of only mutual exclusion, the current density obtained from the mean-field approach is the exact one and as a consequence of this there is a good agreement in results obtained from the mean-field analysis and the Monte Carlo simulation. The mean-field approach, however, does not produce correct results in the presence of additional interactions considered here. This is because the mean-field approach fails to produce even the basic qualitative features of the current density.

In view of these issues, we follow the approach of the hydrodynamic equation [14]. In this approach, we start with the thermodynamic limit, $N\to\infty$ with the lattice spacing $a=l/N\to 0$. For the entire analysis in the following, we choose $l=1$. In the continuum limit, $k\to x=ka$ and $t_{\text{lattice}}\to t=t_{\text{lattice}}a$, the average particle density $\rho(x,t)$ satisfies the continuous version of the continuity equation. With the particle nonconserving terms as additional source and sink terms, we have the continuous equation

$$\frac{\partial\rho}{\partial t}+\frac{\partial}{\partial x}j(\rho)=\Omega_a[1-\rho(x,t)]-\Omega_d\rho(x,t). \tag{6}$$

Here $\Omega_a=\omega_a N$ and $\Omega_d=\omega_d N$. We use the exact stationary current in the hydrodynamic equation with the assumption that the bulk has sufficient time to relax between the particle absorption and desorption events. This is possible when the absorption and desorption happen at a very low rate.

The current density for the interacting system has been derived in the past [10] by using the fact that the stationary distribution is given by the equilibrium distribution of a one-dimensional Ising model. The average current across the bond between k and $k+1$th sites is given by

$$j_k=(1+\delta)\langle 0100\rangle+(1+\Delta)\langle 1100\rangle+(1-\Delta)\langle 0101\rangle + (1-\delta)\langle 1101\rangle, \tag{7}$$

where the four sites in the equation are the $k-1$, k, $k+1$, $k+2$th sites. The four-point averaging needs to be done with respect to the stationary measure. Since the details of the calculations are available in [10], we quote the final result for the current density. In the thermodynamic limit, $N\to\infty$, the current density is

$$j=\frac{\lambda[1+\delta(1-2\rho)]-\Delta\sqrt{4\rho(1-\rho)}}{\lambda^3}, \tag{8}$$

where

$$\lambda=\frac{1}{\sqrt{4\rho(1-\rho)}}+\left(\frac{1}{4\rho(1-\rho)}-1+\frac{1-\Delta}{1+\Delta}\right)^{1/2}. \tag{9}$$

For the mutual exclusion case, $\Delta=\delta=0$, one obtains the exact current density $j=\rho(1-\rho)$. This is also the current density one finds through a mean-field approach starting with $j_k=\langle 10\rangle$. Mean field amounts to ignoring the correlation and assuming $j_k=\langle 1\rangle\langle 0\rangle$. For $\delta=1$ and $\Delta=0$, the current density is $j=2\rho(1-\rho)^2$. The current density vanishes in the completely unoccupied, $\rho\to 0$, and completely occupied, $\rho\to 1$, limits with a maximum at $\rho=1/3$. The lack of the particle-hole symmetry is reflected in the asymmetric nature of the current density around $\rho=1/2$. For $\Delta=1$ and $\delta=0$, the current density is

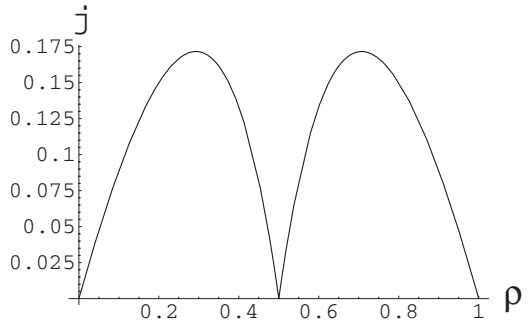

FIG. 2. The plot of the particle current versus particle density for $\delta=0$ and $\Delta=1$.

$$j=y(1-y)/(1+y), \tag{10}$$

where

$$y=\sqrt{1-4\rho(1-\rho)}. \tag{11}$$

The current density is symmetric about $\rho=1/2$, and has two maxima at $\rho=0.707$ and $\rho=0.293$ (see Fig. 2).

Equation (6) is subjected to the boundary conditions $\rho(x=0)=\alpha$ and $\rho(x=1)=\gamma$. Although the first-order equation obtained from Eq. (6) under the steady-state condition, $\partial\rho(x,t)/\partial t=0$, describes the shape of the steady-state density profile as a function of x, this equation, in general, does not have a smooth solution satisfying two boundary conditions. This problem can be overcome by adding a second-order term to this equation. This second-order term is introduced with a prefactor which becomes vanishingly small in the thermodynamic limit. It can be shown that such an infinitesimal second-order term is generated anyway as one takes the continuum limit of (5) and retains terms up to $O(a)$. The second-order term ensures a smooth solution for the hydrodynamic equation through the formation of shocks or boundary layers over a region of width of the order of the lattice spacing, $1/N$. In the steady state, the final form of the equation describing the shape of the density profile is, therefore,

$$\frac{\epsilon}{2}\frac{d^2\rho}{dx^2}-\frac{dj}{dx}+\Omega_a[1-\rho(x)]-\Omega_d\rho(x)=0, \tag{12}$$

where ϵ is a factor of the $O(1/N)$ and $\epsilon\to 0$ in the thermodynamic limit, $N\to\infty$. In the presence of the second-order term, one can define an effective current as

$$J=-\frac{\epsilon}{2}\frac{d\rho}{dx}+j. \tag{13}$$

We discuss later the important role J plays in predicting the nature of the density profile.

A knowledge of certain special densities obtained from Eq. (12) can be useful for us. In the presence of only absorption-desorption kinetics, with $K=\Omega_a/\Omega_d$, the system settles into a stationary density, $\rho=\rho_L=K/(K+1)$ obtained from the zero of the particle nonconserving terms. It is possible for the system to settle into this constant equilibrium density profile in the presence of hopping dynamics also provided the equation of motion allows such a density profile. This is what happens in the case of ASEP with only mutual exclusion. In this case, the current density $j(\rho)=\rho(1-\rho)$ has a maximum $[\,j'(\rho)|_{\rho_m}=0]$ at $\rho=1/2$ and with $K=1$, one has $\rho_L=\rho_m$. This is a very special situation which gives rise to a phase in which the density profile can maintain the maximum current in the system. Thus for $K=1$, in addition to the low-density, high-density, and shock phases one also has a maximal-current phase and coexistence of the maximal-current phase with other phases. Different phases and different exponents associated with the phase transitions in the purely mutual exclusion case indicate the existence of a different universality class for $K=1$. A recent paper [9] shows that instead of the value of K, it is the relative magnitude of ρ_L and ρ_m that determines the phase diagram of the system. While $\rho_L=\rho_m$ (for the purely mutual exclusion case, this condition is fulfilled if $K=1$) forms a special case where the maximal-current phase appears, the phase diagrams for $\rho_L<\rho_m$ and $\rho_L>\rho_m$ are related through the particle-hole symmetry. In our entire analysis, we consider $K=1$ ($\Omega_a=\Omega_d=\Omega$). This, however, does not restrict us to any special universality class as we maintain $\rho_L\neq\rho_m$.

III. BASIC PRINCIPLES OF BOUNDARY LAYER ANALYSIS

We mention here a few basic principles that have been employed in the following boundary layer analysis. We start from the basic hydrodynamic equation (12). Since the contribution of the second-order term in this equation is very small in the thermodynamic limit, it is expected that the major part of the density profile is described by the solution of the first-order equation obtained from Eq. (12) by ignoring the second-order term. This solution, known as the outer solution, cannot satisfy both the boundary conditions in general. In order to satisfy the boundary conditions appropriately, there appear special narrow regions [of width of $O(\epsilon)$] such as boundary layers or shock. In order to see these regions, it is necessary to rescale the position variable of the differential equation appropriately. These regions are described by inner solutions which are solutions of the rescaled equation. Upon rescaling equation (12), the nonconservative terms acquire a prefactor of $O(\epsilon)$, due to which these terms are neglected. The inner solution is, therefore, determined by the first two terms of Eq. (12). Different unknown constants, present in the solutions in different regions, are determined from the boundary conditions or by the conditions required for the smooth joining of the outer and inner solutions. This is the general scheme [15] through which one can obtain a uniform approximation of the solution of Eq. (12) in the thermodynamic limit.

Based on these principles, a few predictions about the presence or absence of the shock in the density profile can be made. The knowledge about the shape of the density profile with shock or the location of the shock, however, requires explicit calculations. Since the particle nonconserving terms of Eq. (12) are not important for the boundary layer or the shock region, we expect the total current J to remain constant in this region. For a shock separating two densities $\rho_{\rm lo}$ and $\rho_{\rm ro}$, we have the total current $J=j(\rho_{\rm lo})$ and $J=j(\rho_{\rm ro})$ at the two edges of the shock and the constancy of the total current J across the shock, demands $j(\rho_{\rm lo})=j(\rho_{\rm ro})$. This condition is implemented explicitly in the boundary layer analysis in finding out the inner solutions describing the shocks or boundary layers. As a consequence of this constancy condition, the path representing the shock on the current density plot is horizontal. For an upward shock in the density profile ($d\rho/dx>0$), one requires $J<j(\rho)$. The horizontal path representing the upward shock on the current density plot must lie below the curve $j(\rho)$. Therefore, we require at least one maximum in the current and density relation to fulfill these conditions for an upward shock. Similarly, we expect $j(\rho)<J$ in case of a downward shock ($d\rho/dx<0$). This requires a concave region in the current versus density plot. In our case, due to the particle-hole symmetry, the center of the downward shock lies at $\rho=1/2$. As a result, $\rho_{\rm lo}$ and $\rho_{\rm ro}$ are bounded as $0.5<\rho_{\rm lo}<0.707$ and $0.293<\rho_{\rm ro}<0.5$. In the boundary layer analysis, these conditions appear naturally as requirements for the saturation of the shock solution (inner solution) to the bulk on both sides of the shock.

IV. BOUNDARY LAYER ANALYSIS FOR $\delta=1$ AND $\Delta=0$

We start our analysis by finding out the outer solutions. The outer solution is the solution of

$$-2(1-4\rho+3\rho^2)\frac{d\rho}{dx}+\Omega(1-2\rho)=0, \tag{14}$$

obtained from Eq. (12) by ignoring the second-order term. The solution is given in terms of the transcendental equation,

$$g(\rho_{\rm out})=\Omega x+c, \tag{15}$$

where

$$g(\rho)=-\tfrac{1}{2}(3\rho^2-5\rho)+\tfrac{1}{4}\ln(2\rho-1) \tag{16}$$

and c is a constant that can be found out from the boundary condition that the outer solution satisfies. As in the pure mutual exclusion case, there can be a phase where the outer solution satisfies the left boundary condition $\rho(x=0)=\alpha$. We consider this situation in the following. In this case, the outer solution is given by

$$g(\rho)=\Omega x+g(\alpha). \tag{17}$$

The inner solution describing the boundary layers or shocks can be found from Eq. (12), by expressing it in terms of $\tilde{x}=(x-x_0)/\epsilon$, where x_0 represents the location of the inner solution. The nonconservative terms in the rescaled equation are negligible in the $\epsilon\to 0$ limit. The inner solution is, therefore, the solution of the equation

$$\frac{1}{2}\frac{d\rho}{d\tilde{x}} = 2(\rho - 2\rho^2 + \rho^3) + C, \tag{18}$$

where C is a constant. The saturation of the inner solution to $\rho_o = \rho_{out}(x \to 1)$ as $\tilde{x} \to -\infty$ is ensured by choosing

$$C = -2(\rho_o - 2\rho_o^2 + \rho_o^3). \tag{19}$$

Equation (18) can be rewritten as

$$\frac{d\rho}{d\tilde{x}} = 4(\rho - \rho_o)(\rho - \rho_1)(\rho - \rho_2), \tag{20}$$

where

$$\rho_{1,2} = \tfrac{1}{2}[2 - \rho_o \pm (4\rho_o - 3\rho_o^2)^{1/2}]. \tag{21}$$

The general solution of Eq. (20) is

$$\ln\left(\frac{(\rho-\rho_o)^{(\rho_1-\rho_2)}(\rho-\rho_1)^{(\rho_2-\rho_o)}}{(\rho-\rho_2)^{(\rho_1-\rho_o)}}\right) = 4(\rho_o-\rho_1)(\rho_o-\rho_2)(\rho_1-\rho_2)(\tilde{x}+\xi), \tag{22}$$

where ξ is a constant. There are possibilities of saturation of the inner solution to densities $\rho_1(\rho_o)$ or $\rho_2(\rho_o)$ as $\tilde{x} \to \infty$. These two densities are functions of α and Ω through ρ_o. The possibility of saturation to ρ_1 can be ruled out since for all values of ρ_o in the range $\{0,1\}$, $\rho_1 > 1$. The inner solution can, however, saturate to ρ_2 which remains in the realistic range (<1) in the entire range of ρ_o. In case of saturation, the approach to ρ_2 is given by

$$\rho \sim \rho_2 + (\rho_2 - \rho_o)^{(\rho_1-\rho_2)/(\rho_1-\rho_o)}(\rho_2-\rho_1)^{(\rho_2-\rho_o)/(\rho_1-\rho_o)} \times \exp[-4(\rho_2-\rho_o)(\rho_1-\rho_2)(\tilde{x}+\xi)]. \tag{23}$$

Two length scales appear in the inner solution. The length scale ξ describes the center of the inner solution. Using the boundary condition, $\rho(\tilde{x}=0)=\gamma$, that Eq. (22) must satisfy, we have

$$\xi = \frac{1}{4(\rho_o-\rho_1)(\rho_o-\rho_2)(\rho_1-\rho_2)} \times \ln\left(\frac{(\gamma-\rho_o)^{\rho_1-\rho_2}(\gamma-\rho_1)^{\rho_2-\rho_o}}{(\gamma-\rho_2)^{\rho_1-\rho_o}}\right). \tag{24}$$

The other length scale, which we denote as w, describes the approach of the inner solution to the saturation value. This length scale is

$$w = 1/[4(\rho_1-\rho_2)(\rho_2-\rho_o)]. \tag{25}$$

This case of outer and inner solutions satisfying the boundary condition at $x=0$ and $x=1$, respectively, is possible for low values of α. This phase, with α dominated bulk density for low values of α is the low-density phase.

The boundary layer at $x=1$ is unable to satisfy the right boundary condition if $\gamma > \rho_2$ and as a consequence of this, the boundary layer deconfines from the boundary at $x=1$ as $\gamma > \rho_2$. To satisfy the right boundary condition, an outer solution joined smoothly to the boundary layer at the left and satisfying the right boundary condition at its right appears. The deconfinement of the boundary layer from the boundary as γ exceeds ρ_2 is the shockening transition that has been seen earlier in the pure mutual exclusion case. The phase boundary between the low-density and the shock phase can be determined from the condition

$$\rho_2(\alpha) = \gamma. \tag{26}$$

As the shock phase boundary is approached the length scale ξ diverges logarithmically as

$$\xi \sim \ln(\gamma - \rho_2). \tag{27}$$

Equation (20) also exhibits a boundary transition that has been first identified as a dual transition in the pure mutual exclusion case [8] and is expected to be present in general whenever there is a bulk shockening transition through a deconfinement of a boundary layer. This boundary transition happens in the low-density phase and across this boundary transition, the slope of the boundary layer (inner solution) changes sign. It can be seen from Eq. (20), that the boundary layer has a positive slope if $\rho_o < \gamma < \rho_2$ and has a negative slope if $\gamma < \rho_o$. Thus, this change in the slope of the boundary layer happens across the boundary transition line

$$\rho_o(\alpha) = \gamma. \tag{28}$$

We call the low-density phase with boundary layer having positive slope as low-density (1). The other part of the low-density phase is called low-density (2). The boundary transition supports the duality theorem of Ref. [8] that for every α if there is a bulk phase transition at $\gamma=\rho_2$, there is a boundary transition at $\gamma=\rho_o(\alpha)$. As the boundary transition line is approached from either side, the length scale ξ diverges logarithmically as

$$\xi \sim \ln(\rho_o - \gamma). \tag{29}$$

The bulk shockening transition line and the boundary transition line meet at a point where

$$\rho_o = \rho_2 = \gamma. \tag{30}$$

This is the critical point at which the length scale w diverges as

$$w \sim \frac{1}{(\rho_2 - \rho_o)}. \tag{31}$$

Equation (30), along with Eq. (21) leads to the critical value for $\gamma_c = 1/3$. The corresponding critical value of α can be determined by implementing the condition $\rho_o(\alpha_c)=1/3$ in Eq. (17). This leads to the following equation:

$$g(1/3) = \Omega + g(\alpha_c), \tag{32}$$

from which the Ω dependent α_c can be determined.

The analysis presented here agrees with the predictions of our earlier work. Although numerical values of α and γ for the critical point or for other transitions are now shifted, the qualitative features of the phase diagrams and phase boundaries remain the same as that of the pure mutual exclusion case with $\Omega_a \neq \Omega_d$. We have shown here that the nature of divergences of different length scales associated with the shock transition and the boundary transition are the same as those in the case of ASEP with only mutual exclusion [7,8].

Since the calculation of other exponents are similar to those of ASEP with only mutual exclusion, we refer the reader to Refs. [7,8] for this purpose.

V. BOUNDARY LAYER ANALYSIS FOR $\delta=0$ AND $\Delta=1$

For $\delta=0$ and $\Delta=1$, we look for those solutions of Eq. (12) which support a downward shock in the density profile. In this system, the downward shock is seen due to the presence of a concave region in the current versus density plot. Due to the particle-hole symmetry, we expect the downward shock to be centered around $\rho=1/2$. Further, there is a discontinuity in $dj/d\rho$ at $\rho=1/2$, because of which we need to distinguish two regions, $\rho>1/2$ and $\rho<1/2$. As a consequence, the boundary layer analysis for the density profile differs significantly from that of the asymmetric case considered in the first part of this paper and also from our previous studies in [7,8].

The bulk solutions on the left and right of the downward shock are described by the left and right outer solutions obtained below. The outer solutions can be obtained by solving Eq. (12) with its first term ignored. The left outer solution, for which $\rho>1/2$, is the solution of

$$-\frac{2(1-2y-y^2)}{(1+y)^2}\frac{d\rho}{dx}+\Omega(1-2\rho)=0, \tag{33}$$

with $y=2\rho-1$. The solution of the equation is

$$g_l(\rho_{\text{lout}})=\Omega x+c_1, \tag{34}$$

where

$$g_l(\rho)=-\frac{1}{\rho}+2\ln\rho-\ln(2\rho-1). \tag{35}$$

c_1 can be fixed from the boundary condition, $\rho(x=0)=\alpha$, since the left outer solution satisfies the left boundary condition.

The equation for the right outer solution can be found out from (12) in a similar way with the substitution $y=1-2\rho$. The right outer solution on the right of the downward shock is

$$g_r(\rho_{\text{rout}})=\Omega x+c_2, \tag{36}$$

where

$$g_r(\rho)=-\frac{1}{\rho-1}-2\ln(\rho-1)+\ln(2\rho-1). \tag{37}$$

As before, c_2 can be determined from the condition $\rho(x=1)=\gamma$. The plot of these two solutions for given α and γ is shown in Fig. 3.

In the following, we find the inner solutions that describe the downward shock. From the symmetry of the current density plot about $\rho=1/2$, we expect the center of the inner solution to correspond to $\rho=1/2$. The inner solution that approaches the left outer solution can be obtained from Eq. (12) with $y=2\rho-1$, after expressing it in terms of $\tilde{x}=(x-x_s)/\epsilon$, where x_s represents the center of the inner solution. With the rescaling of x, the Ω dependent term in Eq. (12) drops out for having negligible contribution. The equation that determines the left inner solution is

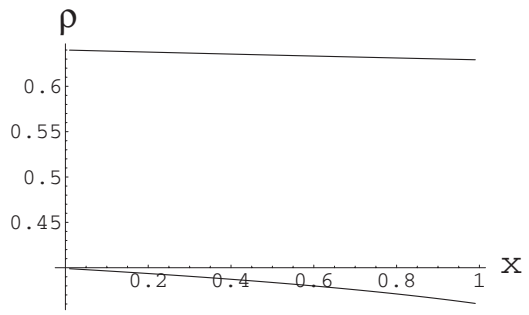

FIG. 3. The plot of the left (upper curve) and right (lower curve) outer solutions. The left outer solution satisfies the left boundary condition $\alpha=0.64$. The right outer solution satisfies the right boundary condition $\gamma=0.36$. We have plotted the solutions until the other end of the lattice.

$$\frac{d\rho}{d\tilde{x}}=-\frac{2+4\rho^2}{\rho}+d_1. \tag{38}$$

We expect the inner solution to saturate to the left outer solution $\rho_{\text{lo}}=\rho_{\text{lout}}(x\to x_s-)$ as $\tilde{x}\to-\infty$. Therefore, we choose

$$d_1=\frac{2+4\rho_{\text{lo}}^2}{\rho_{\text{lo}}}. \tag{39}$$

The solution of (38) is given by the transcendental equation

$$-\frac{\rho_{\text{lo}}^2}{2}\ln(\rho-\rho_{\text{lo}})+\frac{1}{4}\ln(2\rho\rho_{\text{lo}}-1)=(\tilde{x}+c)(2\rho_{\text{lo}}^2-1). \tag{40}$$

The constant c can be found out by demanding $\rho(\tilde{x}=0)=1/2$. The inner solution should approach ρ_{lo} as $\tilde{x}\to-\infty$. This is possible if $2\rho_{\text{lo}}^2-1<0$. Thus on the high-density side, the shock should saturate to a density ρ_{lo} which is bounded as

$$0.707>\rho_{\text{lo}}>0.5. \tag{41}$$

The right inner solution that approaches the right outer solution $\rho_{\text{ro}}=\rho_{\text{rout}}(x\to x_s+)$ as $\tilde{x}\to\infty$ can be found out in a similar way. Substituting $y=1-2\rho$ in Eq. (12), we find the right inner solution

$$\frac{p_{\text{ro}}^2}{2}\ln(p-p_{\text{ro}})-\frac{1}{4}\ln(2pp_{\text{ro}}-1)=(2p_{\text{ro}}^2-1)(\tilde{x}+d), \tag{42}$$

where $p=1-\rho$. The constant d can be found out by demanding that $p=1/2$ at $\tilde{x}=0$. This solution also saturates to ρ_{ro} as $\tilde{x}\to\infty$, with the condition that $2p_{\text{ro}}^2-1<0$. Thus on the low-density side, the shock saturates to a value bounded as

$$0.29<\rho_{\text{ro}}<0.5. \tag{43}$$

Conditions in (41) and (43) are the same as those predicted for a downward shock for the particle conserving interacting systems. The boundary layer analysis presented here shows

that these conditions are necessary for the saturation of the inner solutions.

In the fully symmetric situation ($\delta=0$), the inner solution is centered at $\rho=1/2$. This imposes another constraint

$$\rho_{\rm lo} = 1 - \rho_{\rm ro}. \tag{44}$$

This condition also guarantees the matching of the slopes of the left and right inner solutions at $x=x_s$. Equation (44) allows us to find out the shock positions and the dependence of $\rho_{\rm lo}$ and $\rho_{\rm ro}$ on α and γ. If the shock is formed at $x=x_s$, we have

$$g_{\rm l}(\rho_{\rm lo}) = \Omega x_s + g_{\rm l}(\alpha), \tag{45}$$

$$g_{\rm r}(\rho_{\rm ro}) = \Omega x_s + g_{\rm r}(\gamma) - \Omega. \tag{46}$$

Using Eqs. (45), (46), and (44), we have the final equation,

$$g_{\rm l}(\rho_{\rm lo}) = g_{\rm r}(1-\rho_{\rm lo}) + \Omega + [g_{\rm l}(\alpha) - g_{\rm r}(\gamma)], \tag{47}$$

that determines $\rho_{\rm lo}$. Equation (41) and (47) together set the condition for the formation of the shock. Knowing the value of $\rho_{\rm lo}$ from Eq. (47) for given values of α, β, and Ω, one can find out the height of the shock, $H_{\rm shock}$, from $H_{\rm shock}=\rho_{\rm lo}-\rho_{\rm ro}=2\rho_{\rm lo}-1$ and the location of the shock from Eq. ERROR.

VI. SUMMARY

In this paper, we present a boundary layer analysis for studying the shocks and associated transitions for asymmetric simple exclusion processes of interacting particles. The particles that hop in a particular direction on a finite one-dimensional lattice interact mutually. These interactions are present in addition to the usual mutual exclusion among the particles. We consider two different kinds of interactions. In one case, particles have mutual repulsion. In the other case, particle-hole symmetry is broken by the interaction. We consider these two cases separately since in that case simple analytical solutions for the density profile with shock can be obtained. In addition to these interactions, there are possibilities of attachment (detachment) of particles to (from) the lattice. A steady flow of particles on the lattice is maintained through the injection of particles at one end and withdrawal of particles at the other end at certain rates. We assume that the rates are such that the particle densities at the two ends remain α and γ. Depending on the values of these boundary densities α and γ, the system, in the steady state, can be in different phases. These phases are characterized by the shapes of the particle density profiles across the lattice and the particle-current densities. The hydrodynamic equation that involves the exact current density of the particle conserving system is supplemented with additional particle absorption and desorption terms. In our entire analysis, we choose equal particle absorption and desorption rates. The resulting equation is, then, studied using the techniques of boundary layer analysis to obtain the steady-state density profiles.

In the case where the interaction breaks the particle-hole symmetry, the phase diagram and the phase transitions are qualitatively similar to that of the purely mutual exclusion case with unequal particle absorption-desorption rates. In our interacting system, the particle density profile shows a jump discontinuity or shock from a low value to a high value over an extended region on the α-γ space. As in the case of ASEP with only mutual exclusion, the transition to the shock phase happens through the deconfinement of the boundary layer. Associated to this transition to the shock phase, there is also a dual boundary transition across which the slope of the boundary layer changes sign with the bulk density profile remaining the same. The exponents characterizing various phase transitions are the same as those of the ASEP with only mutual exclusion of particles.

In case of repulsion among the particles, it is known that there exists a downward shock for certain values of the boundary densities. We obtain the analytical form of the density profile that has a downward shock. The solutions describing the shock region in the density profile saturate to the bulk part of the density profile exponentially. This exponential approach is possible if the bulk density at the edges of the shock remains within a certain range. We further obtain conditions on the boundary parameters for having such a downward shock, and also the location and the height of the shock. This work opens up the scope of analyzing more general interacting problems. Even in the absence of any compact closed form analytical solutions for the density profile, the basic principles used in this problem should be applicable in more general cases.

APPENDIX: DENSITY PROFILES AT VARIOUS PHASES AND PHASE DIAGRAM FOR $\delta=1$, $\Delta=0$

In this appendix, we present a few representative plots of the density profile at different phases. The density profile in the low-density phase [low-density (1)] has the shape as given in Fig. 4. Figure 5 shows the deconfined boundary layer as γ is increased from the shock transition value $\gamma=0.43\cdots$ for $\alpha=0.15$.

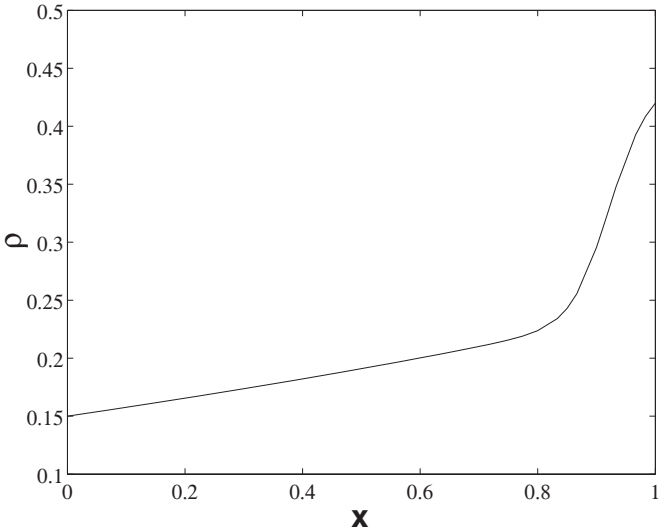

FIG. 4. Plot of the density profile for $\alpha=0.15$, $\gamma=0.42$, $\Omega=0.1$, $\epsilon=0.03$. At these values of the parameters, the system is in the low-density phase, just below shockening transition line.

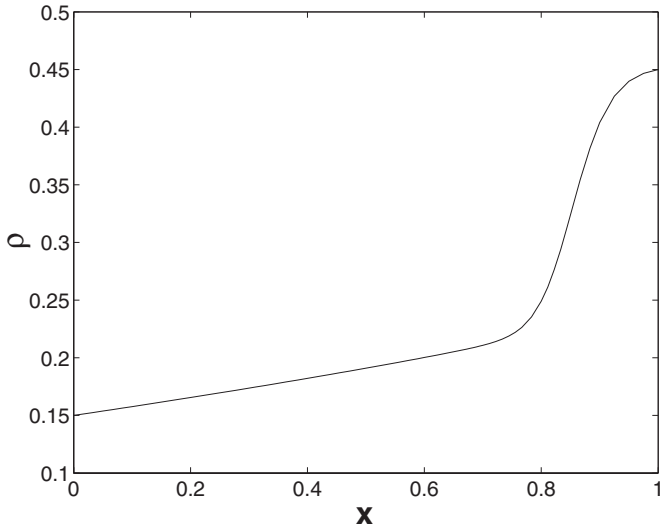

FIG. 5. Plot of the density profile for $\alpha=0.15$, $\gamma=0.45$, $\Omega=0.1$, and $\epsilon=0.03$. At these values of the parameters, the boundary layer is just deconfined from the $x=1$ boundary.

The deconfinement of the boundary layer to form the shock happens only for $\gamma>\gamma_c$. For $\gamma<\gamma_c$, as ρ_o becomes equal to $1/3$ with the increase in α, the shock starts forming with an outer solution appearing on the right of the shock and satisfying an effective right boundary condition $\rho(x=1)=\gamma_c$. The true boundary condition at $x=1$ is satisfied by a decaying boundary layer similar to the one present in the low-density phase. Since for all $\gamma<\gamma_c$, the effective boundary condition on the right for shock formation remains the same, the low-density-shock phase boundary is vertical at $\alpha=\alpha_c$ for $\gamma<1/3$. The shock height increases from zero continuously as one enters the shock phase. The density profile typically appears as in Fig. 6.

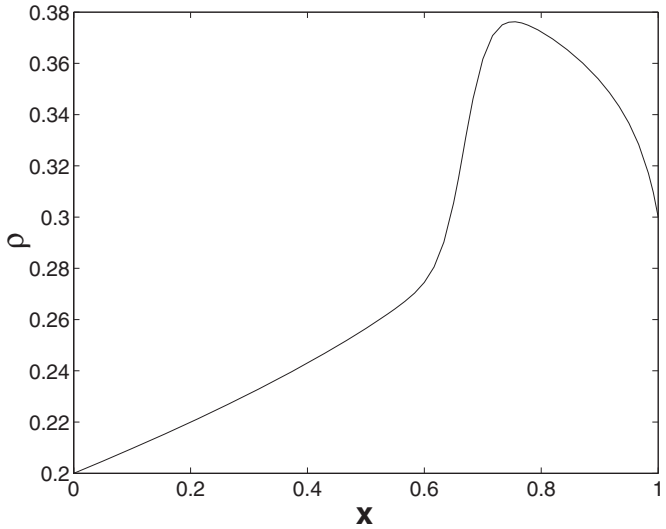

FIG. 6. Plot of the density profile for $\alpha=0.20$, $\gamma=0.30$, $\Omega=0.1$, $\epsilon=0.009$. At these values of parameters, there is a shock in the density profile but it is not formed through the deconfinement of the boundary layer. Two branches of outer solutions are joined discontinuously through the shock whose height increases as α increases with fixed γ.

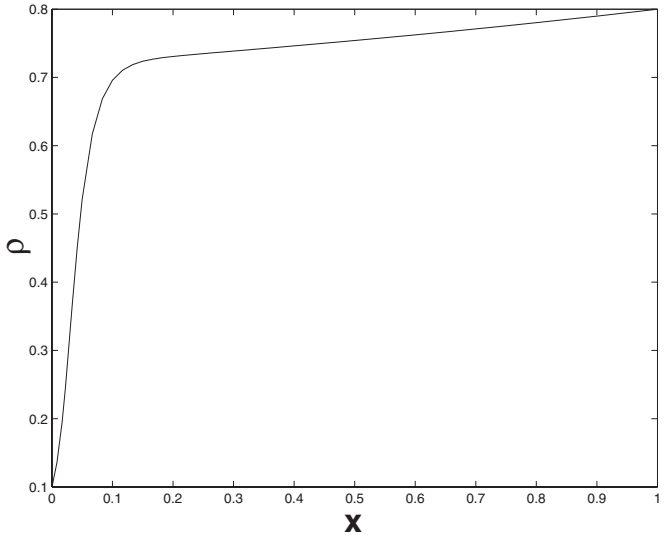

FIG. 7. Plot of the density profile for $\alpha=0.1$, $\gamma=0.8$, $\Omega=0.1$, and $\epsilon=0.034$. At these values of parameters, the system is in the high-density phase.

The shock, after being formed at $x=1$, moves toward the bulk of the system as α is increased for a given $\gamma>\gamma_c$. The shock continues to exist until the other shock phase boundary is reached. At the shock phase boundary, the outer solution satisfying the boundary condition $\rho(x=1)=\gamma$ spans almost the entire lattice except for a narrow region for the inner solution whose saturation value at $x=0$ just matches the boundary density α. With further increase of α, the shock disappears from the system and the system enters into a different phase where there is no shock. The density profile in this phase typically appears as in Fig. 7. Following the case of ASEP with only mutual exclusion, we call this phase the high-density phase. In other words, as we approach the shock phase from the high-density side by decreasing α, the boundary layer deconfines from the $x=0$ boundary in the form of a

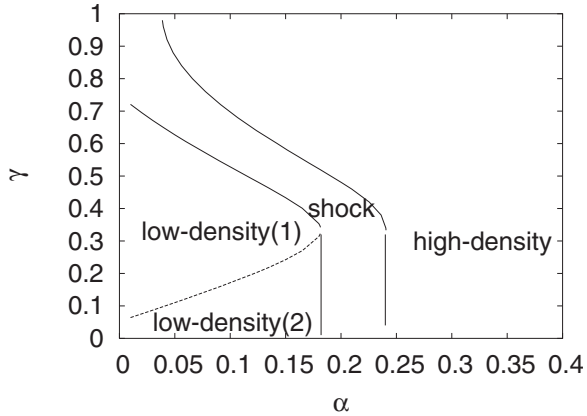

FIG. 8. Quantitative plot of the phase diagram for $\delta=1$, $\Delta=0$, and $\Omega=0.1$. Low-density (1) and low-density (2) are the two low-density phases in which the bulk profiles remain the same but the surface layers have different slopes. These two phases are thus separated by the boundary transition line. The phase boundary between the low-density and shock phases and the boundary transition line meet at the critical point ($\alpha=0.183\cdots$, $\gamma=1/3$).

shock as soon as α becomes smaller than the saturation value of the inner solution at $x=0$. As a result the phase boundary between the shock phase and the high-density phase is given by

$$\rho_2(\rho_o') = \alpha, \tag{A1}$$

where ρ_o' is the value of the outer solution at the boundary $x=0$. Since the outer solution now satisfies the boundary condition at $x=1$, ρ_o' is a function of γ and Ω. The same equation is true for the phase boundary for $\gamma < \gamma_c$ except for the fact that here ρ_o' is independent of γ since $\rho(x=1)=\gamma_c$. This leads to a vertical phase boundary between the shock and the high-density phases. With the phase boundaries specified as above, the phase diagram appears as in Fig. 8. The boundary transition exists in the high-density phase also. Depending on whether the value of α is larger or smaller than ρ_o', the slope of the boundary layer at $x=0$ changes sign. Since the boundary transition lines in the high-density phase can be calculated following the principles mentioned above and also from Ref. [8], we skip those calculations here.

[1] A. Parmeggiani, T. Franosch, and E. Frey, Phys. Rev. Lett. **90**, 086601 (2003); Phys. Rev. E **70**, 046101 (2004).

[2] A. Alberts *et al.*, *The Molecular Biology of the Cell* (Garland, New York, 1994).

[3] S. Klumpp and R. Lipowsky, Europhys. Lett. **66**, 90 (2004); J. Stat. Phys. **113**, 233 (2003).

[4] J. Krug, Phys. Rev. Lett. **67**, 1882 (1991).

[5] B. Derrida *et al.*, J. Phys. A **26**, 1493 (1993); G. Schütz and E. Domany, J. Stat. Phys. **72**, 277 (1993).

[6] M. R. Evans, R. Juhasz, and L. Santen, Phys. Rev. E **68**, 026117 (2003).

[7] Sutapa Mukherji and S. M. Bhattacharjee, J. Phys. A **38**, L285 (2005).

[8] Sutapa Mukherji and Vivek Mishra, Phys. Rev. E **74**, 011116 (2006).

[9] Somendra M. Bhattacharjee, J. Phys. A: Math. Theor. **40**, 1703 (2007).

[10] J. S. Hager, J. Krug, V. Popkov, and G. M. Schutz, Phys. Rev. E **63**, 056110 (2001).

[11] G. M. Schütz, in *Phase Transitions and Critical Phenomena*, edited by C. Domb and J. Lebowitz (Academic, London, 2000), Vol. 19.

[12] A. Kolomeisky *et al.*, J. Phys. A **31**, 6911 (1998).

[13] S. Katz, J. L. Lebowitz and H. Spohn, J. Stat. Phys. **34**, 497 (1984).

[14] V. Popkov, A. Rakos, R. D. Willmann, A. B. Kolomeisky, and G. M. Schutz, Phys. Rev. E **67**, 066117 (2003).

[15] Julian D. Cole, *Perturbation Methods in Applied Mathematics* (Blaisdell, Massachusetts, 1968).